Structure of Liquid $Y_3Al_5O_{12}$ (YAG)

J. K. Richard Weber, Shankar Krishnan, Stuart Ansell,* April D. Hixson, and Paul C. Nordine

Containerless Research, Inc., Evanston, Illinois 60201

(Received 27 September 1999)

The total structure factor $S(Q)$ and the radial distribution function $G(r)$ of liquid $Y_3Al_5O_{12}$ (YAG) were measured at 1770–2230 K by x-ray scattering from samples under containerless conditions in Ar and O_2. Nominal coordination numbers are 4 for Al^{3+} and 6 for Y^{3+} ions. The $G(r)$ has peaks at $r \approx 1.8$ Å for Al-O, $r \approx 2.25$ Å for Y-O, and $r \approx 3.3$–3.6 Å assigned to metal ions in adjacent AlO_4^{5-} and YO_6^{9-} polyhedral ions. Relative to the pure oxides, $G(r)$ for molten YAG has smaller half-widths for the Al-O and Y-O peaks, and an increased sensitivity to temperature and the ambient gas composition.

PACS numbers: 61.20.–p, 61.10.Eq

Experimental research on the structure of molten alumina-yttria compositions is motivated by several factors. These include (i) theoretical interest in analyzing the structure of its component oxides alumina [1–3] and yttria [4,5] by molecular dynamics modeling methods, (ii) observations of phase transition behavior of undercooled alumina-yttria liquids [6,7], and (iii) the technological importance, cf. [8,9], of alumina-yttria materials. There is much information about the properties of the solid phases in this system and nonequilibrium solidification phenomena are well known in connection with melt growth of yttrium aluminum garnet (YAG, $Y_3Al_5O_{12}$) crystals [10,11]. Prior work using NMR techniques showed that the preponderance of four- and six-coordinate aluminum ions in molten calcium aluminate and aluminosilicates is affected by processing conditions and melt composition [12,13]. Recent extended x-ray-absorption fine structure measurements of the Y-O coordination and bond length in liquid YAG [14,15] have stimulated interest in understanding the role of aluminum ion coordination in the complex behavior of this liquid.

The present study extends structure measurements to liquid $Y_3Al_5O_{12}$ over the temperature range 1768–2227 K, up to 470 K below the 2240 K melting point of YAG, and equilibrated with pure Ar and pure O_2 atmospheres.

The high melting point of YAG and the need to investigate the metastable liquid state required the use of a containerless environment to study the structural properties of the liquid. Experiments were performed using a conical nozzle levitation apparatus [16] integrated with x-ray scattering facilities at beam line 12-BM-B at the Advanced Photon Source. The experimental techniques employed for levitation, x-ray scattering, and x-ray data analysis were similar to those used previously [1,4,16,17].

Specimens 0.3 cm in diameter were made from crushed single crystal YAG (Cerac, Inc., Milwaukee, WI) by laser hearth melting, levitated in 0.3–0.4 L/min flows of 4N O_2 or 5N5 Ar and heated with a continuous-wave CO_2 laser beam. The experiments lasted 30–180 min and the specimens lost less than 1% of their initial mass.

Scattering measurements were performed using monochromatic x rays with a photon energy of 14.90 keV, below the fluorescent emission lines of Y. The levitation apparatus was mounted at the center of a six-circle Huber x-ray goniometer so that a small portion of the incident x-ray beam passed over the top of the specimen. Scattering x rays were detected over a 2θ angular range of 10°–110° with an angular resolution ca. 0.5°.

Diffraction data were obtained over Q values [$Q = 4\pi \sin(\theta)/\lambda$] from 1.2–13 $Å^{-1}$. Data were reduced using form factors from Baro *et al.* [18] and the temperature dependence of form factors from Chihara [19]. The data analysis directly yielded the x-ray weighted average structure factor $S(Q)$ which was smoothed using the maximum entropy criterion [20] to reduce ripple. The radial distribution function $G(r)$ was obtained by the inverse Fourier transform method with $G(r)$ constrained to a value of unity at large r. A constant number density of 0.073 atoms/$Å^3$ [21] was used over the experimental temperature range.

Figures 1 and 2 present the x-ray weighted average structure factor $S(Q)$ results for liquid equilibrated with O_2 and Ar at temperatures from just below the melting point of YAG to approximately 470 K below the melting point. The trends are similar in both process atmospheres, deeper undercooling sharpens the first two peaks and shifts the location of the peaks to a lower Q value.

The positions of the peaks in $S(Q)$ were used to classify the ordering in the liquid as proposed by Price *et al.* [22]. The first peak in $G(r)$ represents the nearest-neighbor distance r_1; using a number density of 0.073 $Å^{-3}$, this implies a mean interparticle spacing $d_s = 2.97$ Å. Taking average values for Q_1 and Q_2 of 2.18 and 4.02 $Å^{-1}$, respectively, for all the conditions investigated, and a mean value of $r_1 = 2.02$ Å (average of Al-O and Y-O positions from Table I), the first and second peaks in $S(Q)$ correspond to $(Qr_1, Qd_s) = (4.40, 6.48)$ and $(8.12, 11.94)$. The first two peaks in $S(Q)$ are consistent with chemical short-range ordering and topological short-range ordering, respectively [22].

Figures 3 and 4 present the radial distribution functions $G(r)$. The assigned errors $\delta G(r)$ are the minimum values obtained by error propagation analysis from the structure factor data. The first coordination shell shows two well-resolved peaks near 1.8 and 2.3 Å; these correspond to

 0031-9007/00/84(16)/3622(4)$15.00

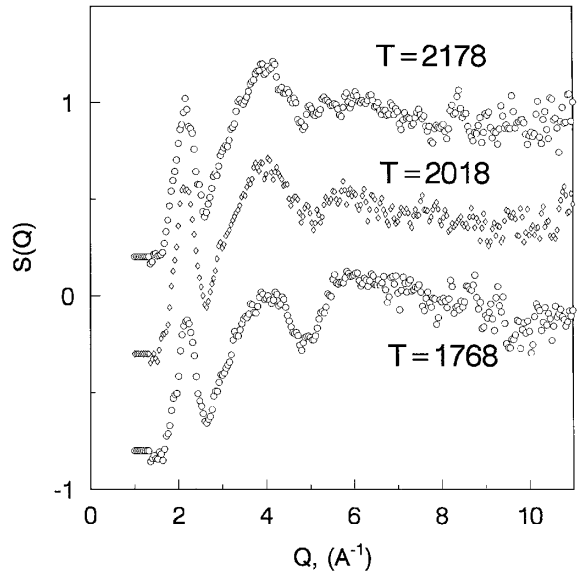

FIG. 1. Total structure factor $S(Q)$ for liquid YAG in O_2 at temperatures of 2178, 2018, and 1768 K. The melting point of YAG is 2243 K. The $S(Q)$ values at 2018 and 1768 K are shifted for clarity.

Al-O and Y-O correlations. Table I summarizes the r values of the two main peaks. The first column lists the experimental temperature; the second and third columns give the Al-O and Y-O bond lengths. We have assigned errors of ± 0.03 Å to the derived values of bond lengths.

A third peak in $G(r)$ occurs around 3.6 Å with additional correlations at larger distances. There is a shoulder on the high-r side of the Y-O peak at the highest temperatures in Ar. This feature moves to larger r values as the temperature is decreased, to merge with the third peak. In O_2, a high-r shoulder on the Y-O peak occurs at the lowest temperature, which becomes a minor peak at $r = 2.7$ Å at higher temperatures.

TABLE I. Results of structural measurements on liquid $Y_3Al_5O_{12}$.

Temperature (K)	Radial distance (Å, ±0.03)		Coordination (±0.5)	
	Al-O	Y-O	Al-O	Y-O
	oxygen atmosphere			
2178	1.80	2.24	4.3	5.5
2018	1.80	2.28	4.5	5.4
1768	1.76	2.24	3.6	6.0
	argon atmosphere			
2227	1.75	2.26	4.0	6.2
2044	1.76	2.28	4.0	5.6
1880	1.84	2.30	5.1	5.1

Values of the mean first-shell coordination were extracted from the $G(r)$ data using a peak reflection procedure. The Al and Y coordinations could be estimated separately because these correlations did not overlap but occurred at distinct radial distances. The first-shell coordinations for Al and Y ions are given in the last two columns in Table I. The absolute values of coordination number are uncertain by ± 0.5 [17], while the relative differences are measured to a higher precision. The correlation between the bond lengths and coordination numbers agrees well with independent experimental measurements [23] and simulations [2,3,5].

In calculating the Y atom coordination, the shoulder area was included at the highest temperature in Ar and the lowest temperature in O_2. Thus, the Y coordination increases as the liquid is undercooled in O_2 and decreases with undercooling in Ar.

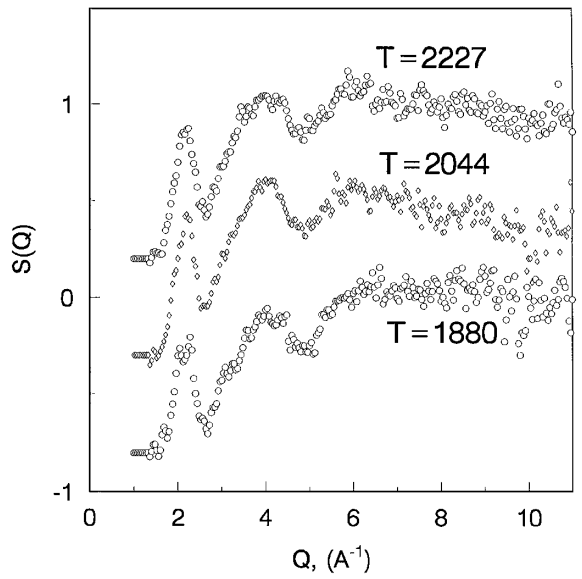

FIG. 2. Total structure factor $S(Q)$ for liquid YAG in Ar at temperatures of 2227, 2044, and 1880 K. The $S(Q)$ values at 2044 and 1880 K are shifted for clarity.

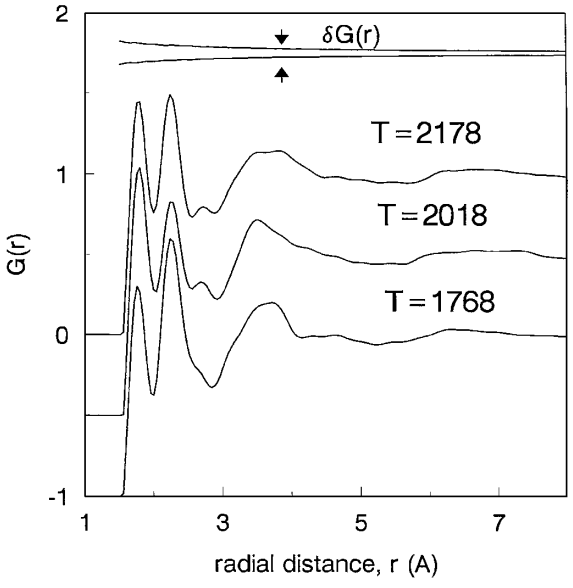

FIG. 3. Radial distribution function $G(r)$ for liquid YAG in O_2 at temperatures of 2178, 2018, and 1768 K. The $G(r)$ curves at 2018 and 1768 K are shifted for clarity. The peaks at $r \approx 1.8$ and 2.25 Å are assigned to Al-O and Y-O, respectively.

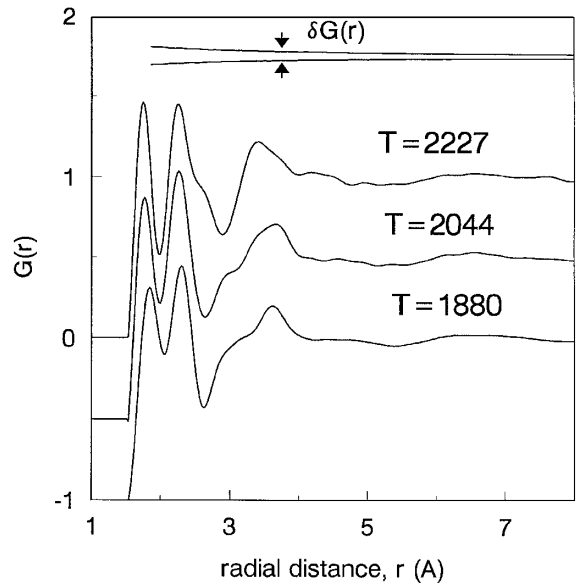

FIG. 4. Radial distribution function $G(r)$ for liquid YAG in Ar at temperatures of 2227, 2044, and 1880 K. The $G(r)$ curves at 2044 and 1880 K are shifted for clarity. The peaks at $r \approx 1.8$ and 2.25 Å are assigned to Al-O and Y-O, respectively.

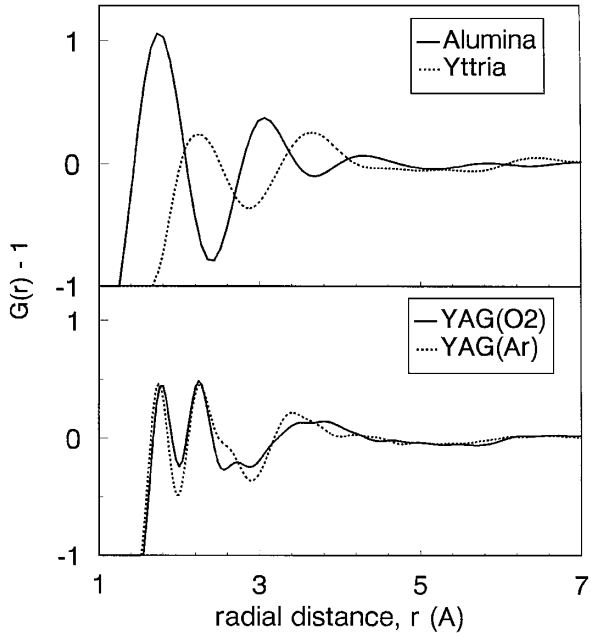

FIG. 5. Comparison of the radial distribution function $G(r)$ for liquid YAG in O_2 and Ar (bottom) with $G(r)$ for pure aluminum oxide and pure yttrium oxide (top). The $G(r)$ results are for the liquids near the respective melting temperatures.

Figure 5 shows $G(r)$ results for liquid $Y_3Al_5O_{12}$ in O_2 in Ar and experimental values for pure liquid Al_2O_3 [1] and Y_2O_3 [4]. The data correspond to the liquids near their respective melting temperatures. Molecular dynamics simulations have also been performed for liquid Al_2O_3 [2,3] and Y_2O_3 [5] in which the partial $G(r)$ data were obtained in reasonable agreement with the experimental results.

Before discussing the structure in $G(r)$ results for molten YAG, we first address the properties of crystalline and molten YAG that provide a context.

Crystalline YAG has a large unit cell with 96 O^{2-} ions, 40 Al^{3+} ions, 24 in fourfold and 16 in sixfold coordination, and 24 Y^{3+} ions in eightfold coordination [24]. The bond distances in the crystal are somewhat larger than the corresponding bonds in the liquid. Nevertheless, a volume increase occurs on melting: the crystal density (at ambient temperature) is 4.55 g/cm^3 [25] and the liquid density is 3.67 g/cm^3 [21] at the melting point. After allowing for thermal expansion of the crystal a large volume increase upon melting remains that is comparable to the 20% volume increase on melting of pure Al_2O_3 [26]. Much open space must exist between the ionic species that occur in the liquid. A disordered assembly of polyhedral AlO_x^{3-2x} and YO_z^{3-2z} ions is a good model for such a liquid.

Liquid YAG has a low viscosity that decreases slowly with temperature at and above the melting point [21]. Between 2240 and 2340 K the viscosity changes by only 14%. The undercooled liquid displays a very large viscosity [27], which increases from about 300 to 3000 P between 1650 and 1600 K and is much larger than the value of ca. 2 P extrapolated from the high temperature measurements. This fragile [28] behavior shows that considerable changes in the structure and bonding can occur when the liquid is undercooled.

Several different phase transitions have been observed in undercooled molten YAG. At cooling rates less than about 200 K/s, a metastable mixture of Al_2O_3 and $YAlO_3$ crystals may be formed or single phase YAG crystals may nucleate [29,30]. A two-phase glass is formed at higher cooling rates [7]. Two-phase glasses have also been obtained from melts of 24–32 mol % yttria in alumina [6].

We now consider the $G(r)$ results for five of the six measurements, excluding the results for deeply undercooled liquid in an Ar gas environment. The first two peaks in the remaining five data sets are at $r = 1.75$–1.80 Å and 2.24–2.28 Å and were assigned to Al-O and Y-O correlations. These peak locations agree with the corresponding values for the pure oxide liquids [1,4] and with the accepted ionic radii [23] of 1.36 to 1.38 Å for O^{2-}, 0.39 Å for four-coordinate Al^{3+}, and 0.90 Å for six-coordinate Y^{3+}.

As seen in Fig. 5, the Al-O and Y-O peaks for molten YAG are quite narrow, and the assigned coordination numbers (see Table I) are in reasonable agreement with four-coordinated Al^{3+} and six-coordinated Y^{3+} ions. Taken together, the results imply that the coordination numbers are more uniform and the polyhedral species are more regular in YAG than in the pure oxides. The results suggest that the predominant species are tetrahedral AlO_4^{5-} and octahedral YO_6^{9-} ions.

As previously discussed the density and bond distance changes on melting of YAG show that the liquid contains much unfilled space between its component polyhedral units. Also, considerable apex and edge connections

must exist between the polyhedral units because stoichiometry requires that the average O^{2-} ion is shared between at least three of these units. It follows that a wide range for Al-Y, Al-Al, and Y-Y correlations is possible. For example, AlO_4 and YO_6 units that share an apex O^{2-} ion may have an Al-Y distance ranging from about 4.0 Å for an axial orientation down to 3.3 Å if the connection is bent. Thus, the broad peak in $G(r)$ at $r \approx 3.3$ to 3.6 Å is assigned to metal-metal correlations in adjacent polyhedral ions. We suggest that the smaller variations in this peak with temperature and environmental conditions result from changes in the intermediate range ordering of the polyhedral species.

Although departure from stoichiometry is small (on the order of a few hundred parts per million), the influence of oxygen content on structure of the liquid can be large due to changes in connectivity of the polyhedra. These changes may result in extended range ordering associated with increased viscosity. Removal of oxygen from the liquid can change the average connectivity of the polyhedral structures, leading to changes in viscosity and tendency to crystallize [6,7,27,29,30].

Now consider the $G(r)$ results for deeply undercooled molten YAG in Ar where the r value for the peak assigned to Al-O increases. The increased bond distance suggests an increased coordination of Al^{3+}. Formation of $AlO_6{}^{9-}$ octahedra is consistent with this change and with the increased coordination number calculated for Al.

In conclusion, we report the first total structure factor $S(Q)$ and radial distribution function $G(r)$ for liquid $Y_3Al_5O_{12}$ over the temperature range 1770–2230 K and equilibrated with pure O_2 and Ar. The $S(Q)$ shows two peaks at 2.18 and 4.0 $Å^{-1}$, consistent with chemical short-range order and topological short-range order. The $G(r)$ shows peaks corresponding to Al-O and Y-O correlations and a broad peak at $r \approx 3.3$–3.6 Å attributed to correlations of metal ions in polyhedral $AlO_4{}^{5-}$ and $YO_6{}^{9-}$ ions joined by shared O^{2-} ions. Relative to pure liquid Al_2O_3 and Y_2O_3, liquid $Y_3Al_5O_{12}$ has more regular polyhedral units, more uniform metal ion coordination, and an increased sensitivity of structural parameters to temperature and the ambient gas chemistry. These results are consistent with reported density, viscosity, and phase transition phenomena in undercooled liquid YAG.

This work was supported by NASA Microgravity Research Division under Contract No. NAS8-40847. Access to the APS beam line was provided by the BESSRC CAT supported by DOE Office of Basic Energy Sciences under Contract No. W-31-109-ENG-38. The authors thank Dr. David Price of Argonne National Laboratory (ANL) for comments and suggestions, Dr. Ricardo Fernandez of ANL, and Dr. Mark Beno and Dr. Jennifer Linton of BESSRC for their help.

*Present address: ESRF, Grenoble, France.

[1] S. Ansell *et al.*, Phys. Rev. Lett. **78**, 464 (1997).
[2] M. A. San Miguel, J. F. Sanz, L. A. Alvarez, and J. A. Odriozola, Phys. Rev. B. **58**, 2369 (1998).
[3] M. Hemmati, M. Wilson, and P. A. Madden, J. Phys. Chem. B **103**, 4023–4028 (1999).
[4] S. Krishnan, S. Ansell, and D. L. Price, J. Am. Ceram. Soc. **81**, 1967 (1998).
[5] L. Alvarez, M. A. San Miguel, and J. A. Odriozola, Phys. Rev. B. **59**, 11 303 (1999).
[6] S. Aasland and P. F. McMillan, Nature (London) **369**, 633–636 (1994).
[7] J. K. R. Weber, A. D. Hixson, J. G. Abadie, P. C. Nordine, and G. A. Jerman, J. Am. Ceram. Soc. (to be published).
[8] Y. Zhou, J. Cryst. Growth **78**, 31–35 (1986).
[9] G. S. Corman, Ceram. Eng. Sci. Proc. **12**, 1745–1766 (1991).
[10] J. S. Abell, I. R. Harris, B. Cockayne, and B. Lent, J. Mater. Sci. **9**, 527–537 (1974).
[11] J. L. Caslavsky and D. J. Viechnicki, J. Mater. Sci. **15**, 1709–1718 (1980).
[12] J. P. Coutures *et al.*, C.R. Acad. Sci. Paris **310,IIb**, 1041–1045 (1990).
[13] D. Massiot, F. Taulelle, and J. P. Coutures, Colloq. Phys. **C5**, 425–431 (1990).
[14] X. Launay *et al.*, C.R. Acad. Sci. Paris **324II**, 527–535 (1997).
[15] C. Landron *et al.*, Europhys. Lett. **44**, 429 (1998).
[16] S. Krishnan *et al.*, Rev. Sci. Instrum. **68**, 3512–3518 (1997).
[17] S. Ansell, S. Krishnan, J. J. Felten, and D. L. Price, J. Phys. Condens. Matter **10**, L73 (1998).
[18] J. Baro, M. Roteta, J. M. Fernandez-Varea, and F. Salvet, Radiat. Phys. Chem. **44**, 531–552 (1994).
[19] J. Chihara, J. Phys. F **17**, 295–304 (1987).
[20] A. K. Soper, Inst. Phys. Conf. Proc. R. Soc. **97**, 711–720 (1989).
[21] V. J. Fratello and C. D. Brandle, J. Cryst. Growth **128**, 1006 (1993).
[22] D. L. Price, S. C. Moss, R. Reijers, M-L. Saboungi, and S. Susman, J. Phys. C. **21**, L1069–L1072 (1988).
[23] R. D. Shannon and C. T. Prewitt, Acta Crystallogr. B **25**, 925–946 (1969).
[24] F. S. Galasso, *Structure and Properties of Inorganic Solids* (Pergamon, Oxford, 1970).
[25] S. J. Schneider, R. S. Roth, and J. L. Waring, J. Res. Natl. Bur. Stand. Sect. A **65**, 345–374 (1961).
[26] P. Tyrolerova and W. K. Lu, J. Am. Ceram. Soc. **52**, 77–79 (1969).
[27] J. K. R. Weber, J. J. Felten, B. Cho, and P. C. Nordine, Nature (London) **393**, 769–771 (1998).
[28] C. A. Angell, Science **267**, 1924–1935 (1995).
[29] M. Gervais, S. LeFloch, N. Gautier, D. Massiot, and J. P. Coutures, Mater. Sci. Eng. B **45**, 108–113 (1997).
[30] I-C. Lin, A. Navrotsky, J. K. R. Weber, and P. C. Nordine, J. Non-Cryst. Solids **243**, 273–276 (1999).